Annals of Nuclear Medicine (2020) 34:884–891
https://doi.org/10.1007/s12149-020-01543-x

ORIGINAL ARTICLE

The quantification of PET–CT radiotracers to determine minimal scan time using quadratic formulation

Mohamad Aminudin Said[1] · Marianie Musarudin[2] · Nur Farahiyah Zulkaffli[2]

Received: 24 February 2020 / Accepted: 6 August 2020 / Published online: 3 November 2020

Abstract

Objective ^{18}F is the most extensively used radioisotope in current clinical practices of PET imaging. This selection is based on the several criteria of pure PET radioisotopes with an optimum half-life, and low positron energy that contributes to a smaller positron range. In addition to ^{18}F, other radioisotopes such as ^{68}Ga and ^{124}I are currently gained much attention with the increase in interest in new PET tracers entering the clinical trials. This study aims to determine the minimal scan time per bed position (T_{min}) for the ^{124}I and ^{68}Ga based on the quantitative differences in PET imaging of ^{68}Ga and ^{124}I relative to ^{18}F.

Methods The European Association of Nuclear Medicine (EANM) procedure guidelines version 2.0 for FDG-PET tumor imaging has adhered for this purpose. A NEMA2012/IEC2008 phantom was filled with tumor to background ratio of 10:1 with the activity concentration of 30 kBq/ml ± 10 and 3 kBq/ml ± 10% for each radioisotope. The phantom was scanned using different acquisition times per bed position (1, 5, 7, 10 and 15 min) to determine the T_{min}. The definition of T_{min} was performed using an image coefficient of variations (COV) of 15%.

Results T_{min} obtained for ^{18}F, ^{68}Ga and ^{124}I were 3.08, 3.24 and 32.93 min, respectively. Quantitative analyses among ^{18}F, ^{68}Ga and ^{124}I images were performed. Signal-to-noise ratio (SNR), contrast recovery coefficients (CRC), and visibility (V_H) are the image quality parameters analysed in this study. Generally, ^{68}Ga and ^{18}F gave better image quality as compared to ^{124}I for all the parameters studied.

Conclusion We have defined T_{min} for ^{18}F, ^{68}Ga and ^{124}I SPECT CT imaging based on NEMA2012/IEC2008 phantom imaging. Despite the long scanning time suggested by T_{min}, improvement in the image quality is acquired especially for ^{124}I. In clinical practice, the long acquisition time, nevertheless, may cause patient discomfort and motion artifact.

Keywords PET quantification · Minimal scan time · ^{18}F · ^{68}Ga · ^{124}I

Introduction

In recent years, the use of ^{18}F-FDG has become a huge success in molecular imaging due to the targeting characteristic of this compound as a marker of glucose metabolism. However, this advantage is not optimal in all types of cancer. ^{18}F-FDG is shown to give low specificity and sensitivity for non-glucose uptake cases. The previously published manuscript stated that ^{18}F-FDG gives a limited role in neuroendocrine tumors (NETs) as the well-differentiated NETs are slow growing and do not avid the ^{18}F [1]. Despite that, the American Thyroid Association (ATA) management guidelines do not recommend the use of ^{18}F-FDG in the evaluation of differentiated thyroid cancer (DTC). This is because the primary lesion of the thyroid cancer might be overlooked [2]. Currently, the limitations of positron emission tomography (PET) imaging with ^{18}F especially in staging and diagnosis of NETs and DTC have been shown to improve with other PET tracers such as ^{68}Ga and ^{124}I.

However, each PET radioisotope consists of different physical properties that give rise to different impacts on PET quantitative imaging as shown in Table 1. For instance, the use of ^{68}Ga might contribute to low spatial resolution and increase of image blurring which is caused by partial volume effect (PVE). Other than that, ^{68}Ga also consists of low positron yield and large positron range in tissue due to its higher positron energy emission. Overall, the PET imaging

✉ Marianie Musarudin
marianie@usm.my

1 Nuclear Medicine Department, Institut Kanser Negara, Putrajaya, Malaysia

2 School of Health Sciences, Health Campus, Universiti Sains Malaysia, 16150 Kubang Kerian, Kelantan, Malaysia

Table 1 The physical properties ^{18}F, ^{68}Ga, and ^{124}I PET radionuclides

Radionuclide	Half-life	Positron yields (%)	Mean positron energy (MeV)	Mean positron range (mm)
^{18}F	109 min	96.9	0.25	0.06
^{68}Ga	68 min	89	0.89	4.4
^{124}I	4.2 days	23	0.82	3.5

quantitative and image quality may be disturbed in such ways.

In addition to ^{68}Ga, ^{124}I with a long half-life yet non-pure positron emitters is another isotope becoming relevant for PET imaging. Regardless of its advantage, the presence of prompt gamma emission that falls within the energy window of the scanner (61% of 605 keV single photon emission of ^{124}I) may contribute to the significance effects like inaccurate measurable of photon detection which eventually caused the rate of true coincidence events detection to decrease [3–5]. Detections of these prompt gamma emissions could either increase or lower the background uniformity, and thus the noise level. Indirectly, these prompt gamma events also affected the dead time of the detector as well as scanner correction. Previously, a higher noise level is reported in a higher background counts and thus leads to the inconsistent radioactivity distribution in lower activity lesions [4].

Hence, these considerations led to the onset idea of this study. In this work, the quantitative differences in PET imaging of ^{68}Ga and ^{124}I relative to ^{18}F were assessed. The quantitative differences among the three radionuclides were used as a benchmarking in the derivation of the minimal scan time, T_{min} for the ^{124}I and ^{68}Ga. The T_{min} for the ^{124}I and ^{68}Ga was determined based on the 15% COV recommended for ^{18}F. ^{18}F is considered as the reference for the comparison as it is required for most of the measurements by the National Electrical Manufacturers Associations (NEMA) standards and the most widely used in PET routine quality control. At the end of the study, quantitative analyses of the image were performed to identify the effectiveness of the T_{min}.

Materials and methods

All data acquisition and analysis were performed using an integrated PET–CT system with bismuth germanium oxide (BGO) crystal (Discovery ST, GE Medical System, Milwaukee, USA) and PMOD 3.7 medical imaging analysis software.

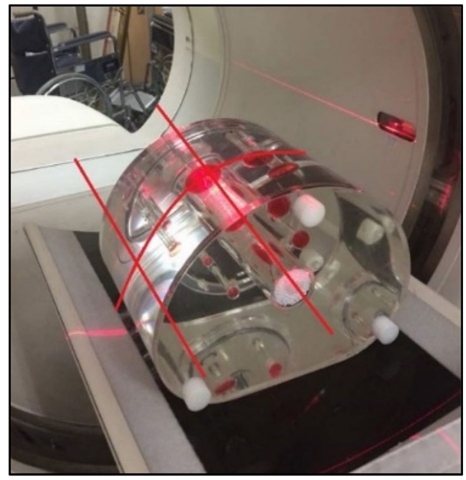

Fig. 1 NEMA2012/IEC2008 phantom positioning on GE Discovery ST PET–CT

PET–CT imaging using NEMA phantom

A NEMA2012/IEC2008 phantom containing six fillable spheres and background compartment was used. The large background compartment was filled with an ^{18}F-FDG solution of 3 kBq/mL. Spheres, representing tumors of 0.50, 1.14, 2.75, 5.65, 11.65, and 27.00 ml, were filled with an ^{18}F-FDG solution of 30 kBq/mL giving tumor background ratio (TBR) of 10:1. A similar amount of ^{68}Ga and ^{124}I activity concentration was filled into the phantom's sphere and background volume. Routine list-mode PET scan time at the one-bed position was implemented in this study. The phantom was placed on the scanner bed with the center of each sphere aligned on the transverse plane and center of the field of view as shown in Fig. 1. Data were acquired for 1, 5, 7, 10 and 15 min acquisition time to determine the T_{min} for each radioisotope. Five PET–CT acquisitions are done for each radionuclide and hence a total of 15 acquisitions performed in this study.

The images were reconstructed using a fully 3D ordered subset expectation maximization (OSEM) algorithm. Two iterations and 21 subsets, with the standard Gaussian post-filters with 6.0 mm full width half maximum (FWHM) were used. OSEM is currently the most widely used iterative reconstruction method [6, 7]. This reconstruction scheme provides better image quality due to the incorporation of correction for geometrical response and detector system efficiency, system dead time, random coincidence, scatter and attenuation [8].

Derivation of T_{min}

T_{min} is used to determine the optimum radioactivity given to the patients using quadratic formulation. Analysis of the coefficient of variations (COV) was used as a platform in the derivation of T_{min}. COV is presenting the variability of the data, i.e. the amount of noise present in an image. The most uniform region in the image, specifically the phantom background usually considered for the COV calculation. COV was determined by the ratio between the standard deviation of the counts in the volume of interest (VOIs) of the background (SD_B) to the mean counts of backgrounds VOIs (M_B) as described in by [9]

$$COV = \frac{SD_B}{M_B}100. \quad (1)$$

In this study, the derivation of T_{min} was performed by fitting the measured COV data using the power-law function. COV data as a function of scan time per bed position was plotted and fitted using the concerning function which is presented by $COV = aT^{-b}$, where T is the scan time per bed position, a and b are the fitting coefficients. As recommended, COV = 15% is considered acceptable to ensure the image quality and quantification accuracy are within tolerance [8]. Therefore, $COV_{max} = 15\%$ was also used as the reference guidelines for ^{68}Ga and ^{124}I in this study. The coefficient determination $R^2 > 0.9$, for all radioisotopes, indicates that the power-law fits the data well. R^2 is commonly presented by values ranging from 0 to 1. It shows how well the fitted data presented the actual data set. R^2 of 1 means that the actual data set is completely explained by the fitted equation. Based on the fitted function, T_{min} can be derived using the following equation:

$$T_{min} = \left(\frac{a}{COV_{max}}\right)^{\frac{1}{b}} \frac{A_B}{3.0}. \quad (2)$$

The A_B described in Eq. 2 is the true activity concentration of the radioisotopes in the background compartment of the phantom during the starting time of the phantom scan T_a. Theoretically, the calculated activity concentration should equal to 3 kBq/ml. COV_{max} of 15% to be used for T_{min} calculation has been previously recommended [8].

Image analysis

To quantify the PET image quality, six spheres inside the phantom image were contoured to define the VOIs. The VOI was defined to include the actual size of the sphere and also corrected for the background uptake. The sphere outlining was done manually with the guidance of CT information (Fig. 2). The previous study did suggest 50, 70% or halfway between background and maximum pixel value for the automatic region of interest (ROI) definition [10]. In this study, the manual definition of VOIs is possible due to the small number of images. The definition of the volume allows the whole volume of the sphere to be analysed in a single analysis. The background

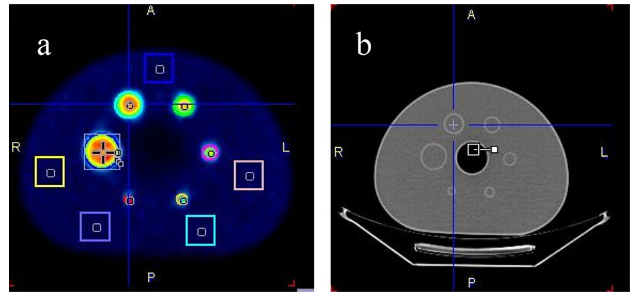

Fig. 2 PET–CT image of NEMA phantom. **a** Axial PET image, **b** axial CT image. The six contoured circles indicate the sphere filled with radioisotopes. The five rectangular shapes represent the background volume

was defined by five rectangular VOIs of 30.0 ml within the background volume.

The image was analysed based on the following parametric:

Contrast recovery coefficient (CRC)

Mathematically, percentage contrast is presented by Eq. 3 [11]. M_S and M_B are the mean concentration (kBq/ml) in the sphere and background each, and R is the true sphere to background activity:concentration ratio (10:1). In an ideal case, the CRC must be equal to 100%.

$$CRC = \frac{\frac{M_S}{M_B} - 1}{R - 1}100. \quad (3)$$

Signal-to-noise ratio (SNR)

SNR is a term used to represent the ratio between signals (meaningful information) to the noise, shown by

$$SNR = \frac{T_S - T_B}{SD_B}, \quad (4)$$

Here T_S and T_B are the total number of counts in sphere VOIs and background VOIs, while SD_B is the standard deviation of background [11].

Visibility (V_H)

Visibility could be defined as the ability to distinguish a hot spot sphere with respect to the background activity concentration, regardless of the sizes of the sphere. Quantitative evaluation of the sphere's visibility is represented by

$$V_H = \frac{M_S - M_B}{SD_B}\sqrt{N_{voxels}}, \quad (5)$$

N_{voxels} is the number of voxels in the spheres [12].

Table 2 COV percentage for ^{18}F, ^{68}Ga, and ^{124}I acquired at 1, 5, 7, 10 and 15 min

Radioisotopes	Acquisition times (min)				
	1	5	7	10	15
^{18}F	26.1	10.4	9.4	8.7	7.4
^{68}Ga	24.7	10.3	10.2	10.5	8.6
^{124}I	79.0	35.5	29.4	27.7	21.2

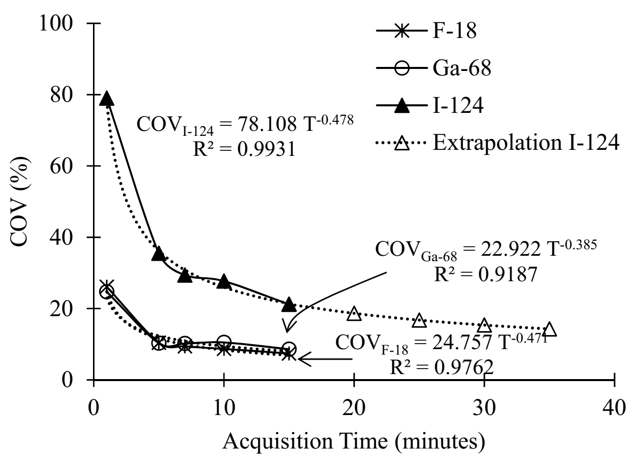

Fig. 3 The COVs measured in the phantom background compartment at several scan durations for ^{18}F, ^{68}Ga, and ^{124}I

Results

Table 2 shows the COV calculated for ^{18}F, ^{124}I and ^{68}Ga, acquired at 1, 5, 7, 10 and 15 min. The COV decreases with the increment of acquisition time for all radioisotopes. The lower value of COV indicates that longer acquisition time leads to a lower degree of variation among the data series. In clinical practice, longer acquisition time nevertheless increases the risk for patient movement, especially for pediatric patients. A comparison of the three radioisotopes reveals that the ^{124}I yielded higher COV as compared to the ^{18}F and ^{68}Ga.

In Fig. 3, the COV against the scan times is presented (the experimental data are shown by the solid lines). The data for ^{18}F, ^{68}Ga, and ^{124}I were fitted using the power-law function with two coefficient variables (the fitted data are shown by the dashed lines). In this study, the power-law resulted in COV equal to 24.757 $T^{-0.471}$, 22.922 $T^{-0.385}$ and 78.108 $T^{-0.478}$ for ^{18}F, ^{68}Ga and ^{124}I, respectively. T in these expressions refers to the scanning time. Noted that, the T_{min} is derived at $COV_{max} = 15\%$ using the derived power-law functions. Alternatively, the derivation of the T_{min} could be performed by interpolation of the fitted COV data [8]. The T_{min} obtained by ^{18}F and ^{68}Ga were 3.08 and 3.24 min, respectively. Meanwhile, the T_{min} for ^{124}I radioisotope was longer than the ^{18}F and ^{68}Ga radioisotopes. At 15 min of acquisition time, the $COV_{I-124} = 21.2\%$, which is still greater than the $COV_{max} = 15\%$ as recommended by the previous study [8]. Hence, extrapolation of the data was performed until it reached the $COV_{max} = 15\%$. Based on the extrapolated data, the T_{min} for ^{124}I is 32.93 min.

Image analyses

Contrast recovery coefficient (CRC)

In Fig. 4, the calculated CRC is plotted against the sphere volume. Noted that, the symbols used to represent ^{18}F, ^{68}Ga, and ^{124}I in Figs. 4, 5, and 6 are consistent throughout this article. Hence, for the simplicity of the figures, we thus added the figure legend in sub-figure (a) only. Comparison agrees that the increment of the acquisition time does not improve the image quality for all radioisotopes assessed (maximum standard deviation of 0.07 was calculated). Therefore, the results presented here are limited to 1 and 5 min of acquisition time. The other data are purposely not presented here due to the insignificant difference. While a small relative difference was calculated between ^{18}F and ^{68}Ga, ^{124}I consistently yields lower CRC as compared to ^{18}F and ^{68}Ga. Overall, the analyses of the small sphere gave lower CRC compares to the larger sphere. Imaging of ^{18}F and ^{68}Ga using the suggested T_{min} do not significantly affect the CRC of these two radioisotopes, with relative differences of 0.19–0.68 and 0.39–1.76%, respectively. Nevertheless, the implementation of T_{min} for ^{124}I leads to significant changes. The CRC obtained from ^{124}I imaging using T_{min} acquisition time is approaching CRC obtained by ^{18}F and ^{68}Ga (Fig. 4c, d).

Signal-to-noise ratio (SNR)

In contrast to CRC, an increment of acquisition time leads to a greater increment of the SNR (highest standard deviation of 13.2, 6.8 and 5.0 for the largest sphere of ^{18}F, ^{68}Ga and ^{124}I each). As expected, image noise for ^{68}Ga is higher and ^{124}I consistently resulted in the lowest SNR value. A comparison shows that the SNR obtained for ^{124}I at 15 min acquisition time equivalent to ^{18}F and ^{68}Ga SNR value acquired at 1 min acquisition time (shown by a thick arrow in Fig. 5c, d). Extrapolation of the data suggested that the acquisition of ^{124}I using calculated T_{min} able to improve the SNR up to 31.6 for the largest sphere and 9.2 for the smallest sphere.

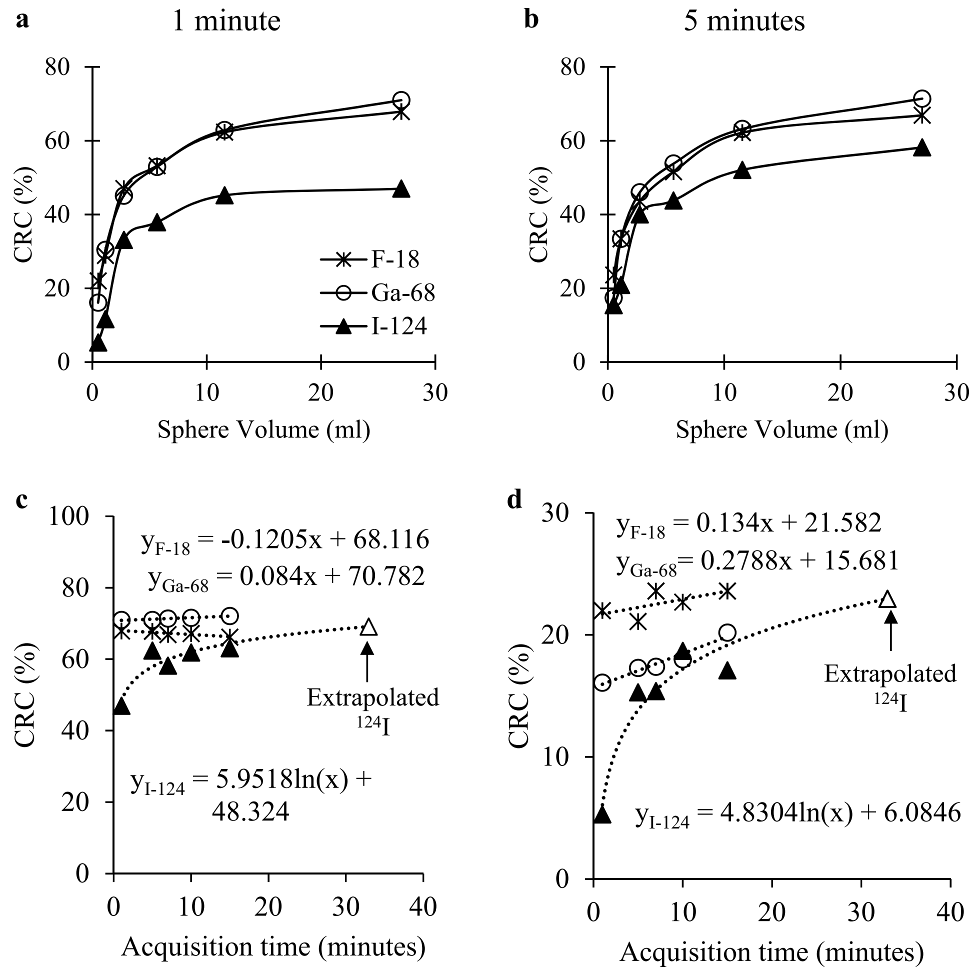

Fig. 4 Comparison of CRC calculated among ^{18}F, ^{68}Ga and ^{124}I, acquired at **a** 1-min, **b** 5-min scanning time. Below: The fitted functions of the CRC measured at several scan durations for ^{18}F, ^{68}Ga and ^{124}I in different spheres volume **c** 27.00-ml sphere, **d** 0.50-ml sphere

Visibility (V_H)

The ability of PET–CT in visualizing small tumors is undeniable. In this study, all radioisotopes show good visibility even for the smallest sphere and shortest acquisition time. These findings nevertheless are limited to the high TBR (TBR = 10:1) tested in this study. Low accumulation of activity (lower TBR) is most likely to show a lower V_H and hence worth being assessed in a future study. According to the Rose criterion, the hot spheres were visible when the V_H value is larger than four [12]. The visibility of the sphere was even better with the usage of ^{18}F, whereby $V_H = 45$ was measured at 1 min acquisition time. In general, ^{68}Ga shows higher V_H compared to ^{18}F at shorter acquisition time, while contrast findings were observed for acquisition time greater than 7 min (Fig. 6). Again, implementation of the T_{min} able to reduce the quantitative difference in the visibility of the sphere especially for the ^{124}I.

Discussion

Limited role of ^{18}F-FDG in NETs due to slow growth of well-differentiated NETs, as well as DTC, has been improved with other PET tracers such as ^{68}Ga and ^{124}I. The different physical properties of the radioisotopes may signify the need for explicit imaging protocol for each radioisotope. In our center, 2-min scanning time per bed position is currently implemented and considered satisfactory for ^{18}F and ^{68}Ga PET–CT imaging. Meanwhile, 20 min is implemented for ^{124}I PET–CT imaging to obtain a satisfactory result. Accordingly, in this study, we attempt to define a T_{min} for each radioisotope commonly used in imaging at our institution. This definition was made based on the quadratic dose formulation previously proposed by another researcher [8]. It should be noted that all images used for the quantification were reconstructed using a Gaussian filter of the same strength. An optimal smoothing filter

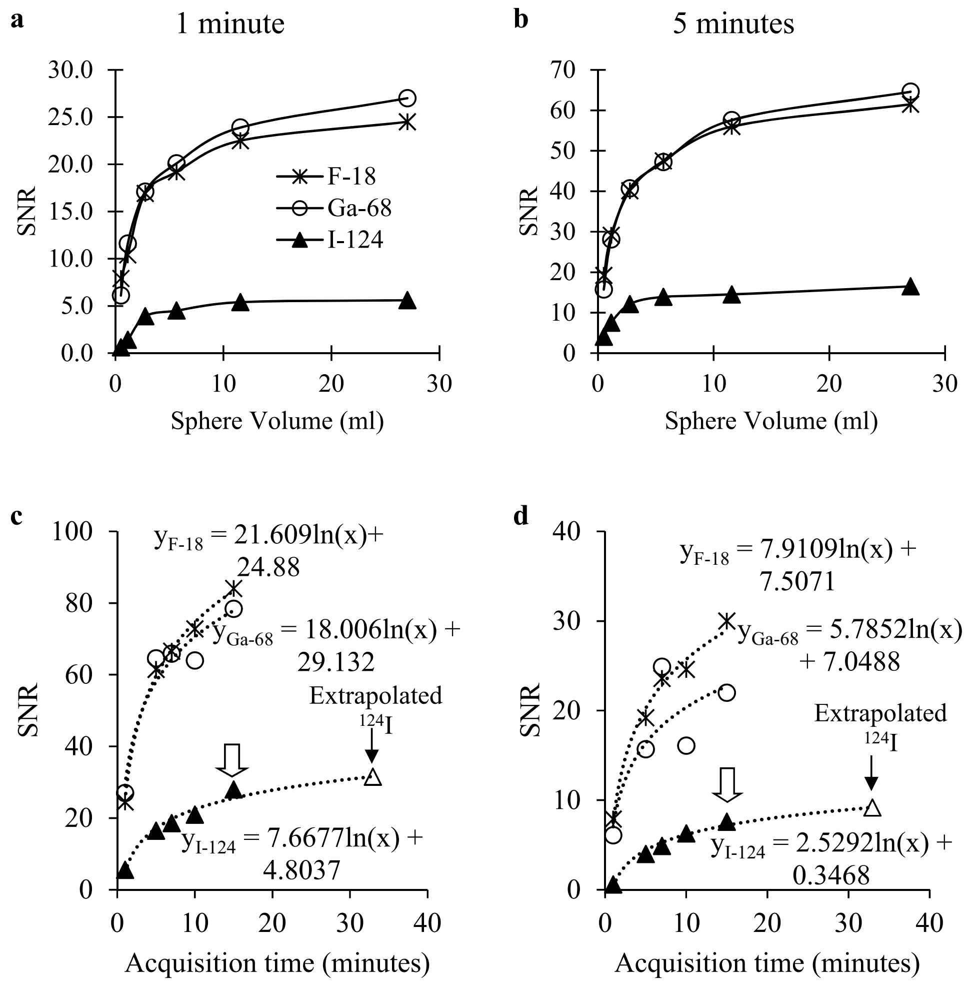

Fig. 5 Comparison of SNR calculated among ^{18}F, ^{68}Ga and ^{124}I, acquired at **a** 1-min, **b** 5-min scanning time. The fitted functions of the SNR measured at several scan durations for ^{18}F, ^{68}Ga and ^{124}I in different sphere's volume **c** 27.00-ml sphere, **d** 0.50-ml sphere

based on the noise level for each image was not performed and thus should be regarded as the limitation of this study.

Using the quadratic dose formulation described by Koopman et al. [8], the suggested T_{min} for ^{18}F and ^{68}Ga is 3.08 and 3.24 min, respectively. These data show that, instead of administered a higher radioactive dose to the patient (as implemented in linear dose protocol), we can improve the PET–CT image quality by lengthening the scanning time up to the T_{min}. For instance, in a linear dose protocol, a 50 kg patient will be administered with 250 MBq of ^{18}F-FDG activity. Rather, an activity as low as 205.2 MBq is appropriate for the same weight of patients when the quadratic dose protocol is implemented [13]. This lower activity will be compensated by longer scanning time as suggested by the T_{min}.

Studies have shown that the ^{124}I ($T_{1/2}$ = 4.18 days) led to longer T_{min} as compared to the current practice in our institution. Extrapolation of the data suggested that 32.93 min scanning time is appropriate for optimal ^{124}I imaging. This scanning time is approximately 65% longer than the current protocol. This is apparently due to the lower positron percentage that caused a longer time needed for ^{124}I scanning acquisition. Though the number of photons per unit time of ^{124}I (23%) and ^{18}F (96.7%) is about four times, the T_{min} for ^{124}I is almost ten times longer compares to the ^{18}F. For ^{124}I, noted that only 23% positron yields possibly used for imaging. Therefore, the low number of annihilation could be compensated by increasing the scanning time up to T_{min}. The possible reason for a longer T_{min} of ^{124}I could be due to the less statistical counts and the positron physical property whereby the energy from the ^{124}I is higher than the energy of ^{18}F. The higher energy of ^{124}I leads to a larger positron range of the isotope. Unfortunately, in clinical practice, the long acquisition time may increase the risk for patient discomfort and consequently motion artifact. Nevertheless, the data proved that the longer image acquisition of the ^{124}I using 15% COV would produce an image contrast (CRC) that is comparable to the ^{18}F and ^{68}Ga images (shown in Table 3; Fig. 4c), as measured on 27.00-ml sphere. For the 0.5-ml sphere, the implementation of T_{min} able to result in better CRC for ^{124}I compares to ^{18}F and ^{68}Ga imaging. Extrapolation of the ^{124}I data at T_{min} gave CRC of 23.0, as tabulated in Table 3. It is worth noted that analyses of the small sphere could be affected by the PVE, whereby underestimation of

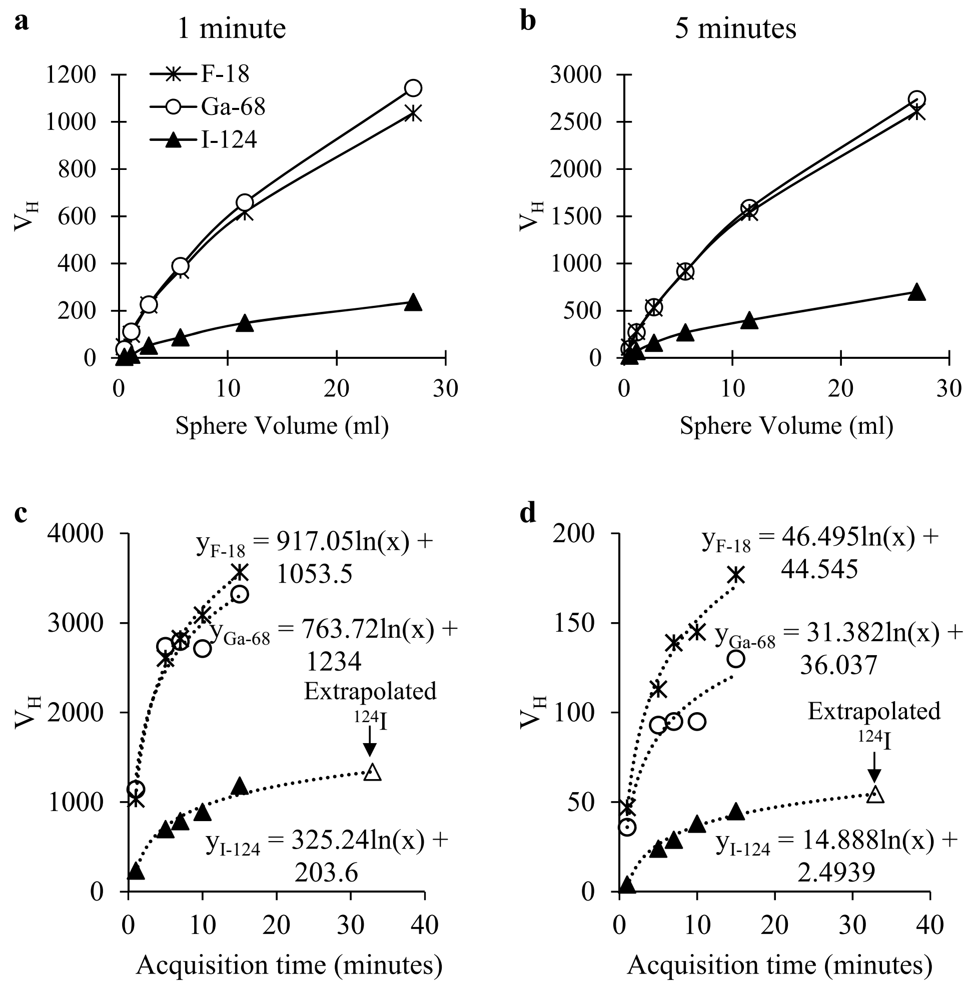

Fig. 6 Comparison of V_H calculated among ^{18}F, ^{68}Ga and ^{124}I, acquired at **a** 1-min, **b** 5-min scanning time. The fitted functions of the V_H measured at several scan durations for ^{18}F, ^{68}Ga and ^{124}I in different spheres volume **c** 27.00-ml sphere, **d** 0.50-ml sphere

Table 3 Comparison of image quantification derived by inter- or extrapolation of the fitted functions at T_{min}

Radioisotopes	Current scanning time (minutes)	T_{min} (minutes)	Image quantification					
			27.00-ml sphere			0.50-ml sphere		
			CRC	SNR	V_H	CRC	SNR	V_H
^{18}F	2	3.08	67.7	49.2	2085	21.2	16.4	97.0
^{68}Ga	2	3.24	71.3	50.3	2131	17.0	13.8	73.0
^{124}I	20	32.93	69.1	31.6	1340	23.0	9.2	54.5

the uptake value may occur [14]. Meanwhile, appropriate improvement of the SNR (13.8 and 15.9% for 27.00- and 0.5-ml sphere each, as shown in Fig. 5c, d) and visibility (13.8 and 15.8% for 27.00- and 0.5-ml sphere each, Fig. 6c, d) compares to the current image acquisition protocol practices in our institution are noted. Nevertheless, this increase is not as good as ^{18}F as it is limited by the standard deviation of the background. For both SNR and visibility of ^{18}F, improvement of 23.4 and 26.3% was noted for the 27.00- and 0.5-ml sphere, respectively. At early scanning time, the higher standard deviation of the background of ^{124}I due to the less counting is a factor affected the SNR and visibility. SNR, which measures the useful signal with respect to the noise is affected by the uncertainty of the counts. Longer acquisition time leads to more data counted, which eventually reduces the background noise. Higher image noise for ^{68}Ga is apparently due to 0.034% of single photon emission in the range of 350–650 keV and 3% of high-energy photon emission (1077 keV). It should be noted that the data presented here are limited to phantom-based imaging using the BGO-based PET–CT system, whereby the other factors like the patient's movement are not taken into consideration.

Conclusion

NEMA2012/IEC2008 body phantom imaging was performed to determine the T_{min} for the ^{124}I and ^{68}Ga based on the quantitative differences in PET imaging of ^{68}Ga and ^{124}I relative to ^{18}F. It was derived based on the recommendation by Boellard et al. for ^{18}F T_{min} calculation, whereby COV_{max} of 15% was used for the calculation [8]. In this study, the T_{min} obtained for ^{18}F, ^{68}Ga and ^{124}I were 3.08, 3.24 and 32.93 min, respectively. Analyses of the images show that imaging of ^{18}F and ^{68}Ga using the suggested T_{min} able to yield CRC that is comparable to the CRC yielded by longer acquisition time. In addition to that, the quantitative difference in the visibility of the sphere was reduced, especially for the ^{124}I. Even though a longer acquisition time has been shown able to improve the SNR, the SNR measured on the image acquired using T_{min} meets the criteria of good image quality according to recommendations of Fukukita et al. [15]. Despite the long T_{min} defined for ^{124}I, extrapolation of the data showed promising improvement in the ^{124}I image quality acquired using the T_{min}. The CRC for the ^{124}I was even approaching the CRC calculated for ^{18}F and ^{68}Ga if the imaging is performing using the T_{min}. In clinical practice, the long acquisition time, nevertheless, may cause patient discomfort and eventually susceptibility to the motion artifact.

Acknowledgements Authors wish to acknowledge the support, succour, and cooperation given by the staff at the Nuclear Medicine Department, Institut Kanser Negara for the data information and also to Universiti Sains Malaysia, Kubang Kerian for supporting this research. This study reference NMRR-19-508-46863 had not funded by any organisation. We would like to thank the Director General of Health Malaysia for his permission to publish this article.

Funding None.

Compliance with ethical standards

Conflict of interest The authors declare that they have no conflict of interest.

References

1. Jessica EM, James RH. Imaging in neuroendocrine tumors: an update for the clinician. Int J Endocr Oncol. 2015;2(2):159–68.
2. Wimmer I, Pichler R. Thyroid cancer: advances in diagnosis and therapy FDG PET in thyroid cancer. London: IntechOpen; 2016.
3. Conti M, Eriksson L. Physics of pure and non-pure positron emitters for PET: a review and a discussion. EJNMMI Phys. 2016;3(1):8.
4. Lubberink M, Herzog H. Quantitative imaging of ^{124}I and ^{86}Y with PET. Eur J Nucl Med Mol Imaging. 2011;38(Suppl 1):S10–8.
5. Disselhorst JA, Brom M, Laverman P, Slump CH, Boerman OC, Oyen WJ, et al. Image-quality assessment for several positron emitters using the NEMA NU 4–2008 standards in the Siemens Inveon small-animal PET scanner. J Nucl Med. 2010;51(4):610–7.
6. Boellaard R. PET imaging instrumentation and principles of PET protocol optimisation. In: Principles and practice of PET/CT: Part 1. A technologist's guide. European Association of Nuclear Medicine 2010. https://www.eanm.org/publications/technologists-guide/principles-practice-petct-part-1/. Accessed 10 June 2018.
7. Tong S, Alessio AM, Kinahan PE. Image reconstruction for PET/CT scanners: past achievement and future challenges. Imaging Med. 2010;2(5):529–45.
8. Koopman D, van Osch JAC, Jager PL, Tenbergen CJA, Knollema S, Slump CH, et al. Technical note: how to determine the FDG activity for tumour PET imaging that satisfies European guidelines. EJNMMI Phys. 2016;3(1):22.
9. Buvat I, Frey E, Green A, Ljungberg M. Quantitative nuclear medicine imaging: concepts, requirements and methods. Human health reports. Vienna: International Atomic Energy Agency; 2014.
10. Boellaard R, Krak NC, Hoekstra OS, Lammertsma AA. Effects of noise, image resolution, and ROI definition on the accuracy of standard uptake values: a simulation study. J Nucl Med. 2004;45:1519–27.
11. Ziegler S, Jakoby BW, Braun H, Paulus DH, Quick HH. NEMA image quality phantom measurements and attenuation correction in integrated PET/MR hybrid imaging. EJNMMI Phys. 2015;2(1):18.
12. Elschot M, Vermolen BJ, Lam MG, de Keizer B, van den Bosch MA, de Jong HW. Quantitative comparison of PET and Bremsstrahlung SPECT for imaging the in vivo yttrium-90 microsphere distribution after liver radioembolization. PLoS ONE. 2013;8(2):e55742.
13. Soret M, Bacharach SL, Buvat I. Partial-volume effect in PET tumor imaging. J Nucl Med. 2007;48(6):932–45.
14. Musarudin M, Muhammad SSH, Said M. Implementation of quadratic dose protocol for ^{18}F-FDG whole-body PET imaging using a BGO-based PET/CT scanner, GE Discovery ST. Iran J Nucl Med. 2019;27(2):73–80.
15. Fukukita H, Suzuki K, Matsumoto K, Terauchi T, Daisaki H, Ikari Y, et al. Japanese guideline for the oncology FDG-PET/CT data acquisition protocol: synopsis of version 2.0. Ann Nucl Med. 2014;28:693–705.